

AD-A045 208

AMPEX CORP REDWOOD CITY CA ADVANCED TECHNOLOGY DIV F/G 13/9
FOIL BEARING INVESTIGATION. NUMERICAL SOLUTION OF THE PLANAR HY--ETC(U)
AUG 77 A ESHL N00014-77-C-0021
RR-77-07 NL

UNCLASSIFIED

| OF |
AD
A045 208



END
DATE
FILMED
11-77
DDC



MICROCOPY RESOLUTION TEST CHART
NATIONAL BUREAU OF STANDARDS-1963-A

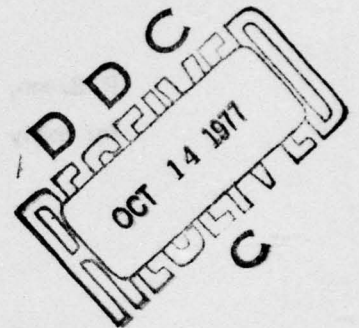
ADA 045208

FOIL BEARING INVESTIGATION

Numerical Solution of the
Planar Hydrostatic Foil Bearing

Prepared Under: Contract No. N00014-77-C-0021
Task NR 062-297
Office of Naval Research

Administered by: Scientific Officer
Mathematical and Information Sciences Division
Office of Naval Research
800 North Quincy Street
Mr. Stanley W. Doroff, Code 438
Arlington, Virginia 22217



Prepared By: *A. Eshel*
A. Eshel
Member of the Research Staff

Approved By: *F. K. Orcutt*
F. K. Orcutt
Manager, Mechanics Section
M. Wildmann
M. Wildmann,
Manager, Research Department

REPRODUCTION IN WHOLE OR IN PART IS PERMITTED FOR ANY PURPOSE OF THE UNITED STATES GOVERNMENT.

THIS DOCUMENT HAS BEEN APPROVED FOR PUBLIC RELEASE; ITS DISTRIBUTION IS UNLIMITED.

ACKNOWLEDGMENT

The foundation of the precompiler were designed by the author as a term project at Stanford University, Computer Science Department, under the guidance of Prof. J. Olinger.

The author is indebted to the above mentioned as well as to Mr. P. Szego, former Mechanics Section Manager, Mr. M. Wildmann and Mr. F. K. Orcutt for many discussions and suggestions.

ACCESS for		
NTIS	File Section	<input checked="" type="checkbox"/>
DDC	B.H. Section	<input type="checkbox"/>
UNANNOUNCED		<input type="checkbox"/>
J.S.I.		
BY		
DISTRIBUTION/AVAILABILITY CODES		
Dist		SPECIAL
A		

RECORDING Tapes FROM FILMED

TABLE OF CONTENTS

	Page
Abstract	1
Nomenclature	2
Introduction	3
Hydrostatic Foil Bearing Model	5
Results and Discussion	9
Appendix I: Preprocessor Solution - Purpose of Preprocessor	15
Formulation	17
Precompiler Input	19
Precompiler Structure	21
Appendix II: O.D.E. Solution	23
Appendix III: Listing of Computer Program Generated by Precompiler	25
References	27
Distribution List	28

ABSTRACT

8

The steady state problem of the planar hydrostatic foil bearing is analyzed and solved numerically. Two techniques of solution are used. One method is simulation in time with asymptotic approach to steady state. This is achieved by a preprocessor which automatically sets up the numerical computer program. The second method is an iterative shooting technique. The results agree well with one another. Curves of pressure and typical film thickness versus flow are presented.

NOMENCLATURE

G	constant found from the solution of Eqn. (25)
h	local film thickness
\bar{h}	dimensionless film thickness h/r_o
\bar{h}_a	dimensionless distance of foil asymptote to cylinder
H	stretched film thickness coordinate
\bar{H}, \hat{H}	auxiliary normalized values of H for computational purposes
m, n	exponents, to be determined
p	local pressure in film
p_a	ambient pressure
Q	volume flow rate per unit bearing width
R	local radius of curvature
r_o	cylinder radius
t	time
T	foil tension per unit width
ϵ	$\frac{12\mu Q}{r_o T}$ dimensionless flow rate
μ	gas viscosity
Π	dimensionless pressure
θ	angular coordinate (origin at point of tangency)
τ	dimensionless time
ξ	stretched angular coordinate
$\bar{\xi}, \hat{\xi}$	auxiliary normalized values of ξ for computational purposes

Subscripts

c	pertains to cylinder center
g	pertains to source location (groove)
t	pertains to point of tangency
∞	pertains to end of lubrication zone

INTRODUCTION

Despite considerable effort in the field of foil bearings over the past two decades, an analysis of hydrostatic foil bearings has not been published. This problem is of interest in magnetic recording and elsewhere. The purpose of this report is to fill this gap.

The initial goal of this investigation was, actually, to illustrate the applicability of a preprocessor computer program for the automatic solution of partial differential equations. Ironically, it turned out, the automatic solution was only partly successful and numerical difficulties were encountered in certain parameter ranges, requiring some human intervention. Consequently, an alternative approach was utilized and a complete set of data curves generated. It is felt, however, that the numerical experience gained in this effort as well as the concepts of the preprocessor are of interest and, therefore, they are reported here as well as the solution of the particular problem at hand.

HYDROSTATIC FOIL BEARING MODEL

Let the configuration shown in Figure 1 be studied. Here, an infinitely wide, hydrostatic, cylindrical, perfectly flexible foil bearing with incompressible lubricant is depicted schematically. In this configuration, one line feed source is located at $\theta = \theta_g$. A second line source is symmetrically situated at the other side of the bearing. It is assumed that the feed pressure p_g is prescribed and maintained constant. The film thickness and pressure are, then, governed by the following differential equations:

$$\frac{\partial}{\partial \theta} \left(h^3 \frac{\partial p}{\partial \theta} \right) = 12 \mu r_o^2 \frac{\partial h}{\partial t} \tag{1}$$

$$p - p_a = \frac{T}{R} = \frac{T}{r_o} \left(1 - \frac{1}{r_o} \frac{\partial^2 h}{\partial \theta^2} + \dots \right) \tag{2}$$

Using the dimensionless representation

$$\bar{h} = \frac{h}{r_o}$$

$$\bar{p} = \frac{p - p_a}{T/r_o}$$

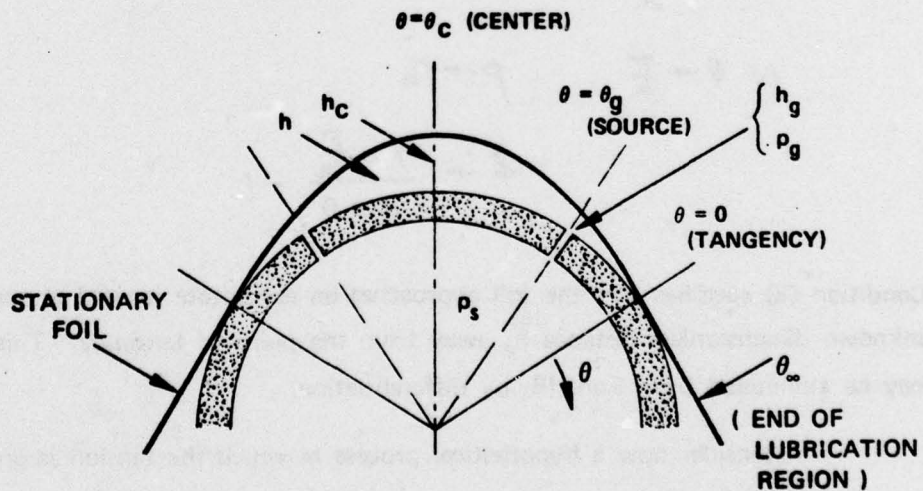


Figure 1 Cylindrical Hydrostatic Foil Bearing

and restricting the problem to steady state, Eqns (1), (2) may be rewritten as

$$\bar{h}^3 \frac{\partial \Pi}{\partial \theta} = -\frac{12\mu Q}{r_o T} \quad (3)$$

$$\Pi = 1 - \frac{\partial^2 \bar{h}}{\partial \theta^2} + \dots \quad (4)$$

where Q is an integration constant representing the volume flow rate per unit width.

Eqns. (3), (4) may be combined to:

$$\bar{h}^3 \frac{\partial^3 \bar{h}}{\partial \theta^3} = \epsilon + \dots \quad (5)$$

where the dimensionless flow rate ϵ is defined by

$$\epsilon = \frac{12\mu Q}{r_o T}$$

It may be observed that under steady conditions there is no flow in the region $\theta_c \leq \theta < \theta_g$ (due to symmetry we restrict our treatment to one half of the problem). The pressure in this region is, therefore, uniformly $p=p_g$. In dimensionless form:

$$\Pi = \Pi_g = \frac{p_g - p_a}{T/r_o}$$

The boundary conditions are:

$$\text{At } \theta = \theta_g \quad \bar{h}, \bar{h}' \text{ and } \Pi \text{ are continuous} \quad (6)$$

$$\text{As } \theta \rightarrow \frac{\pi}{2} \quad p \rightarrow p_a \quad (7)$$

$$\bar{h} \rightarrow \frac{1 + \bar{h}_a}{\cos \theta} - 1 \quad (8)$$

Condition (8) specifies that the foil approaches an asymptote located at some small unknown dimensionless distance \bar{h}_a away from the point of tangency. This unknown may be eliminated from Eqn. (8) by differentiation.

Consider now a hypothetical process in which the tension is gradually increased while $\theta_c, \theta_g, p_g - p_a, r_o, \mu$ remain unchanged. One anticipates a corresponding

reduction of flow, or of ϵ . (Note that this process implies either a change in restriction or in the source pressure, to maintain a constant p_g despite changes in Q). Following a derivation analogous to Ref [1] one assumes

$$H = \frac{\bar{h}}{\epsilon^n} \tag{9}$$

$$\xi = \frac{\theta}{\epsilon^m} \tag{10}$$

The following requirements may be imposed: The two sides of Eqn (5) must balance as $\epsilon \rightarrow 0$; hence,

$$4n - 3m = 1 \tag{11}$$

Secondly, at least one variable term in Eqn (2) must not vanish as $\epsilon \rightarrow 0$; hence,

$$n - 2m = 0 \tag{12}$$

It follows then, that

$$m = 1/5 \tag{13}$$

$$n = 2/5 \tag{14}$$

Thus, in the region

$$\xi_c \leq \xi < \xi_g$$

$$\frac{d^2 H}{d\xi^2} = 1 - \sqrt{1-g} \tag{15}$$

$$\frac{dH}{d\xi} = (1 - \sqrt{1-g})(\xi - \xi_c) \tag{16}$$

$$H = \frac{1}{2}(1 - \pi_g)(\xi - \xi_c)^2 + H_c \quad (17)$$

where H_c is the unknown dimensionless film thickness at $\xi = \xi_c$

The formulation of the problem in region $\theta_g < \theta$ becomes

$$H^3 \frac{d^3 H}{d \xi^3} = 1 \quad (18)$$

$$\left. \frac{dH}{d\xi} \right|_{\xi=\xi_g} = (1 - \pi_g)(\xi_g - \xi_c) \quad (19)$$

$$\left. \frac{d^2 H}{d \xi^2} \right|_{\xi=\xi_g} = 1 - \pi_g \quad (20)$$

$$\left. \frac{dH}{d\xi} \right|_{\xi \rightarrow \infty} \sim \xi \quad (21)$$

$$\left. \frac{d^2 H}{d \xi^2} \right|_{\xi \rightarrow \infty} \sim 1 \quad (22)$$

The fact that we have four boundary conditions for a third order equation indicates that one of the parameters of the problem is not free. The following functional form is, therefore, deduced:

$$\pi_g = f\left(\frac{\theta_g}{\theta_c}, \xi_c\right) \quad (23)$$

$$H = f(\xi; \frac{\theta_g}{\theta_c}, \theta_c) \quad (24)$$

The solution techniques are discussed in the Appendix.

RESULTS AND DISCUSSION

The results are summarized in Figures 2-5. They are expressed in terms of two dimensionless parameters, namely: θ_g/θ_c specifying the source location, and $\left(\frac{12\mu Q}{r_o T}\right)^{1/5}/|\theta_o|$ describing flow rate. Figure 2 illustrates some typical tape contours while Figures 3-5 present the dimensionless groove pressure and some characteristic film thicknesses.

The basic behavior of the bearing as it appears from these graphs may be described by means of a conceptual experiment. In this experiment, $p_g - p_a$ is slowly increased while the geometry and tension remain constant. Initially, when the pressure is low, there is no flow ($Q=0$). When $p_g - p_a$ is increased just above the threshold level of T/r_o , the tape lifts off and starts forming into a "bubble" shape (Figure 2). This contour is typified by a large ratio of h_c/h_t , but the vanishingly small values of both h_c and h_t make the radius of curvature over the source equal to r_o . Increase in pressure above the threshold results in growth of h_c as well as h_t and formation of smaller radius of curvature over the source. The rate of growth of h_c is slower than that of h_t , resulting in a gradual loss of the "bubble" shape. Hence, the radius of curvature over the groove reaches a minimum and then starts growing, eventually exceeding r_o . This growth causes the impedance of the bearing to decrease and the flow to increase. The greater radius of curvature implies, however, that, at the same time, the pressure required to support the foil tension is smaller. The above behavior results in the unexpected phenomenon that the same value of p_g generates two distinct flow rates. This should not be surprising, however, if one remembers that the shape of the flow channel, formed by the foil, is markedly different in the two cases.

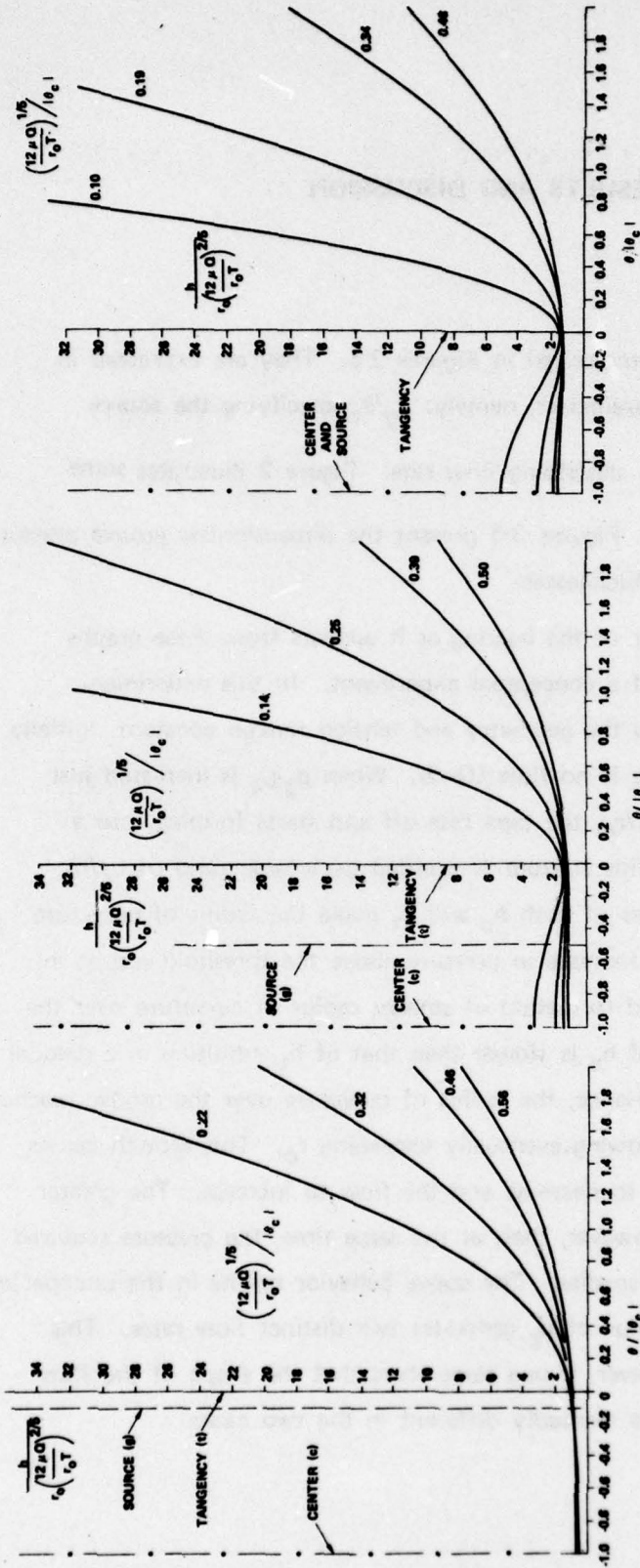


Figure 2c

Figure 2b

Figure 2a

Figure 2a Tape Contours for a Range of Flow Rates With $\theta_g/\theta_c \approx 0.1$

Figure 2b Tape Contours for a Range of Flow Rates With $\theta_g/\theta_c = 0.5$

Figure 2c Tape Contours for a Range of Flow Rates With $\theta_g/\theta_c = 1.0$

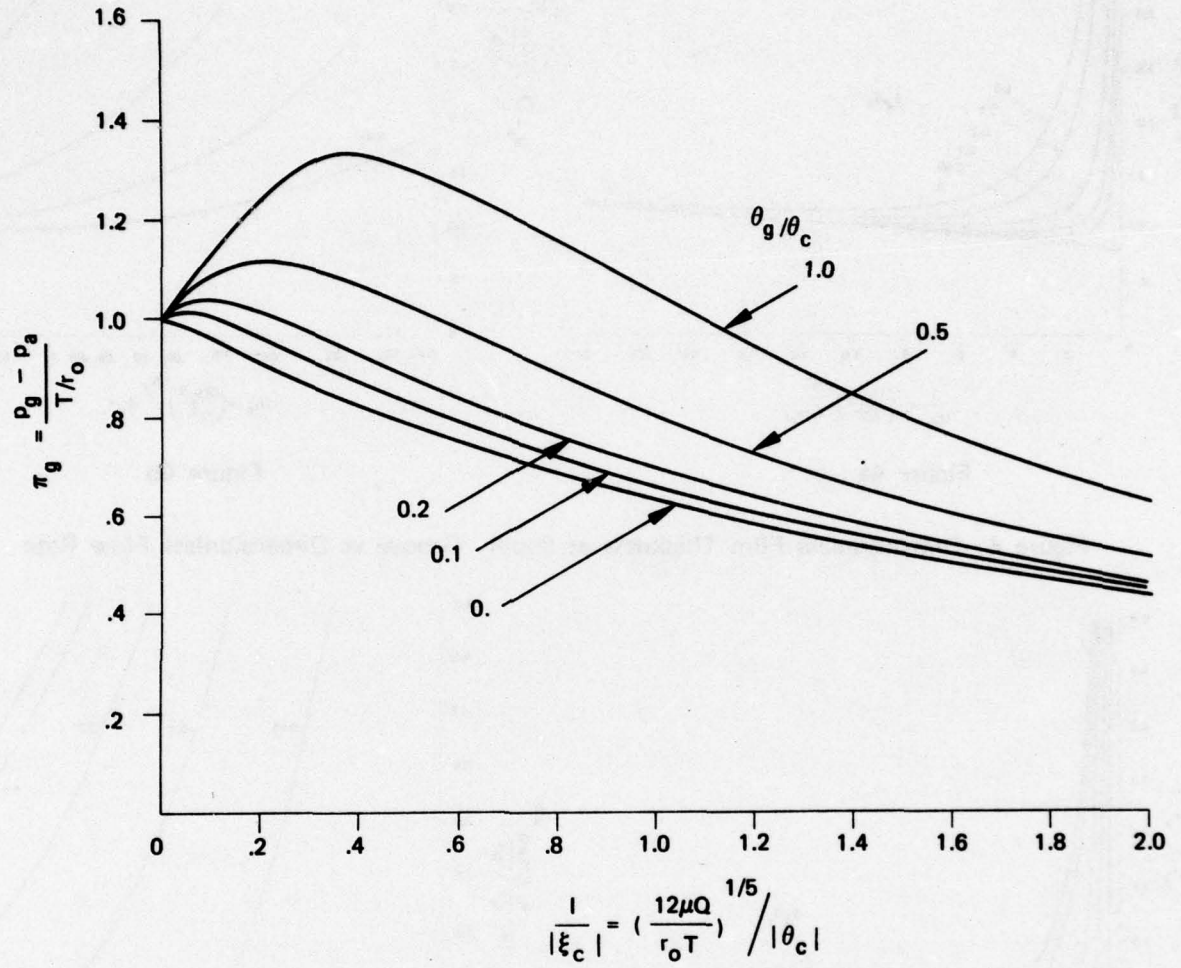


Figure 3 Dimensionless Pressure Drop vs Dimensionless Flow Rate Across Foil Bearing

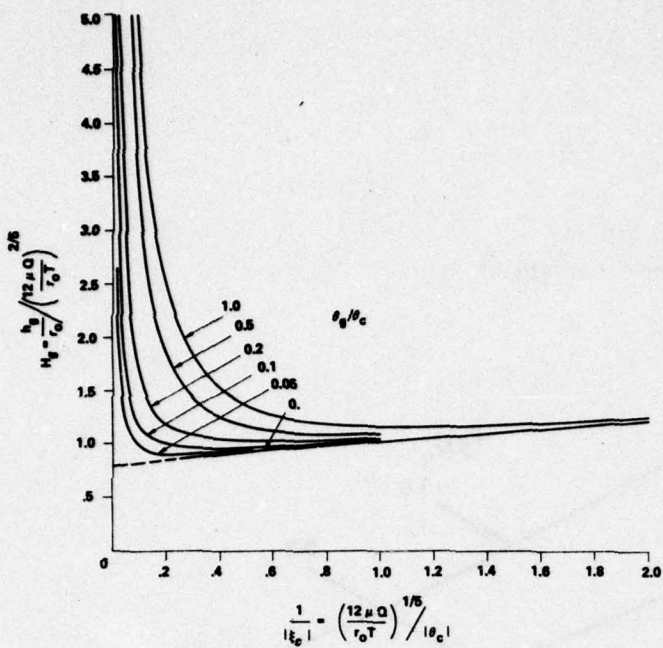


Figure 4a

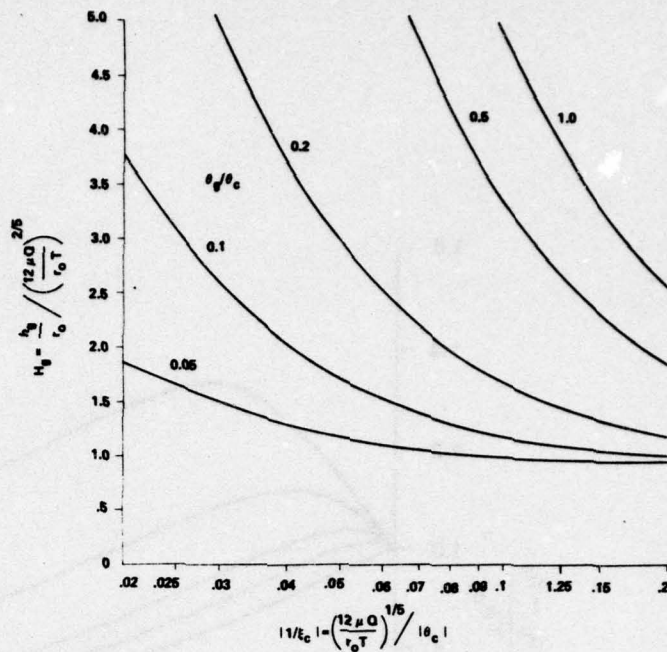


Figure 4b

Figure 4 Dimensionless Film Thickness at Supply Groove vs Dimensionless Flow Rate

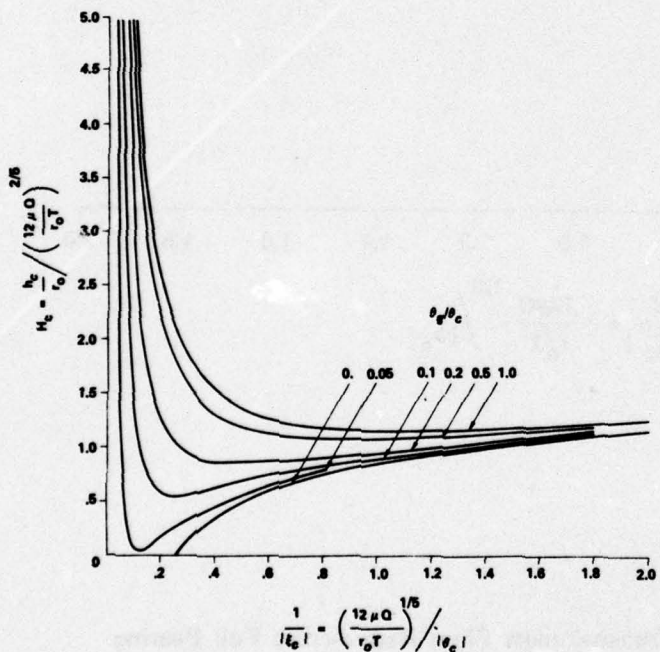


Figure 5a

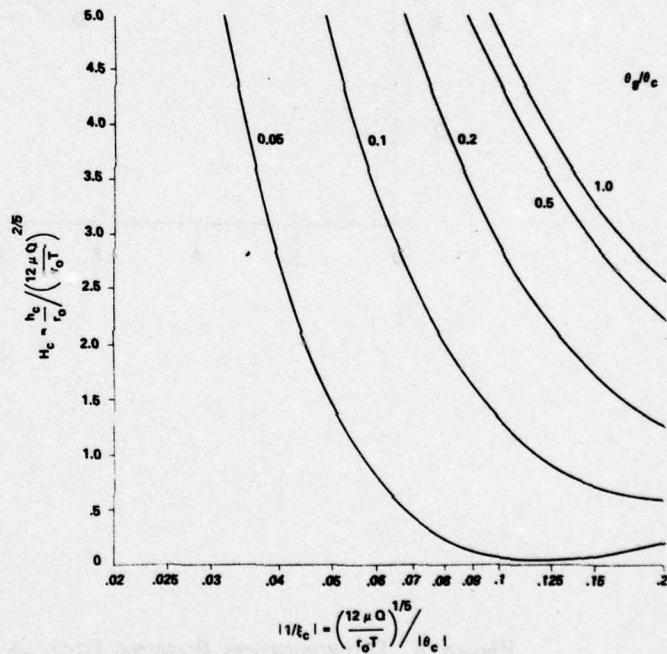


Figure 5b

Figure 5 Dimensionless Film Thickness at Cylinder Center vs Dimensionless Flow

A natural question which arises, is what flow rate will the physical system select in view of the ambiguity. The analysis in this work, determines only the static equilibrium conditions and not their stability and, therefore, cannot provide a complete answer to the question. Nevertheless, a limited insight will be provided in the following discussion.

At the onset let it be noted that the assumption has been implicitly made, that p_g may be controlled independently of Q . In any practical situation the restrictor characteristic presents a curve of p_g vs. Q , which may be superimposed on Figure 3. The intersection determines possible operating points which are schematically illustrated in Figure 6.

Neglecting the effect of damping which may be brought out only by a dynamic analysis, it may be shown that intersections of type A, C tend to be stable whereas intersections of type B tend to be unstable. The argument is essentially as follows. Considering point B for example, a downward fluctuation in p_g causes the bearing outflow to exceed the supply through the restrictor. This tends to push the operating point further down from B by causing a deficiency in fluid at the bearing inlet. Thus, for an intersection of restrictor characteristic and film characteristic such as that shown at B, a disturbance in p_g away from the equilibrium point results in a further excursion of the operating point in the same direction. However, for intersections of types A or C, disturbances in p_g from the equilibrium point result in a restorative effect, suggesting stability.

Another observation of interest is that $\theta_g/\theta_c \approx 0.05$ is a threshold value, below which contact between the tape and the cylinder may arise. In these situations the source is located too close to the point of tangency for useful operation. When the flow is minute, a noncontact situation is possible. For slightly higher flow rates, the seal effect at the tangency point disappears and flotation of the foil cannot be maintained throughout the wrap angle.

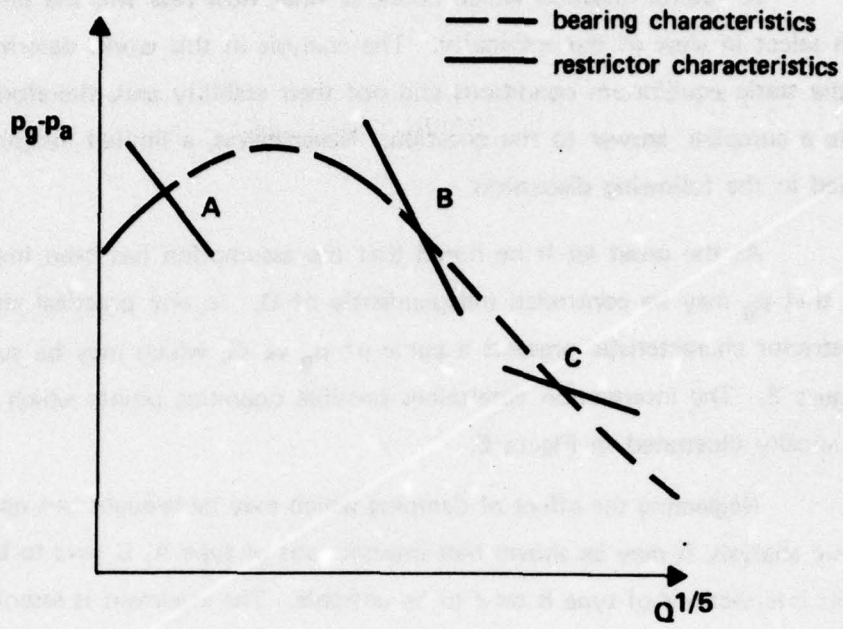


Figure 6 Schematic View of Various Possibilities of Operating Points

APPENDIX I: PREPROCESSOR SOLUTION

PURPOSE OF PREPROCESSOR

With present-day powerful computers, the engineer has at his disposal an invaluable tool for optimization and evaluation of design parameters. Frequently, this evaluation is based on numerical simulation of the behavior of a physical model represented by a partial differential equation (PDE). In order to perform the simulation, it becomes necessary, in such cases, to discretize the partial differential equation (PDE) and to write a computer program that will solve the resulting difference equation and print or display the results numerically and/or graphically. This task is, often, time-consuming and usually requires several debugging runs.

Though laborious, this programming effort, commonly, consists of rather similar subtasks. In general, the programming job may be described as the insertion of problem dependent details into a basic program template designed for the particular algorithm and a broad class of equations. Consequently, it is feasible to carry out this process, too, with the aid of the computer. This is done by means of a preprocessor or a precompiler. The precompiler is a computer program which accepts an input describing the partial differential equation and its boundary conditions in a concise and readable mathematical symbolism, and outputs a high level language (e.g., PLI) program which is then compiled by the language compiler just like a human-written program. The compiler-generated object program is finally executed. (Figure A1).

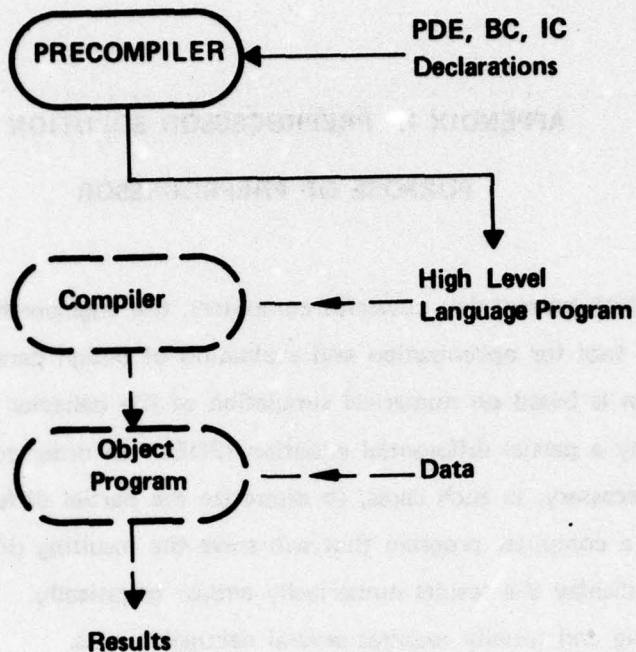


Figure A1 Schematic View of the Role of the Precompiler in Problem Solution. (Broken lines indicate conventional computer solution. Solid lines add the effect of the precompiler.)

In this report, we would limit the discussion to a precompiler for the class of parabolic, high order, one dimensional partial differential equations. We will restrict ourselves, further, to the implicit solution algorithm. This class of problems is still rather broad; and in particular, it is applicable to many foil-bearing problems.

FORMULATION

In order to allow solution by means of a program generated by our precompiler for parabolic partial differential equations, the formulation (18) - (22) for H and Π_g will be replaced by the following alternative formulation defining a function $\bar{H}(\bar{\xi}, \tau)$. \bar{H} will later be transformed to the desired function H (ξ).

$$-\frac{\partial^4 \bar{H}}{\partial \bar{\xi}^4} \cdot \bar{H}^3 - \frac{\partial^2 \bar{H}}{\partial \bar{\xi}^2} \cdot 3\bar{H}^2 \frac{\partial \bar{H}}{\partial \bar{\xi}} = \frac{\partial \bar{H}}{\partial \tau} \tag{25}$$

$$\bar{H} \Big|_{\bar{\xi} = \bar{\xi}_g} = \bar{H}_g \tag{26}$$

$$\frac{\partial \bar{H}}{\partial \bar{\xi}^2} \cdot (\bar{\xi}_g - \bar{\xi}_c) - \frac{\partial \bar{H}}{\partial \bar{\xi}} \Big|_{\bar{\xi} = \bar{\xi}_g} = 0 \tag{27}$$

$$\frac{\partial \bar{H}}{\partial \bar{\xi}} \Big|_{\bar{\xi} = \bar{\xi}_c} \sim \bar{M} \tag{28}$$

$$\frac{\partial^2 \bar{H}}{\partial \bar{\xi}^2} \Big|_{\bar{\xi} = \bar{\xi}_c} \sim 1 \tag{29}$$

When a steady state solution, $\bar{H}(\bar{\xi}; \frac{\bar{M}}{\bar{\xi}_c}, \bar{\xi}_c, \bar{H}_g)$ satisfying these requirements is obtained, a parameter G, elaborated upon later, may be evaluated from

$$G = \bar{H}^3 \frac{\partial^2 \bar{H}}{\partial \bar{\xi}^2} \tag{30}$$

$H(\xi), H_c, \xi_c$ and π_g may then be obtained from the numerical solution obtained by the transformations

$$H = \bar{H}/G^{4/5} \tag{31}$$

$$\xi = \bar{\xi}/G^{1/5} \tag{32}$$

$$\pi_g = 1 - \left. \frac{\partial^2 \bar{H}}{\partial \bar{\xi}^2} \right|_{\bar{\xi} = \bar{\xi}_g} \tag{33}$$

$$H_c = \bar{H}_g - \frac{1}{2}(1 - \pi_g)(\bar{\xi}_g - \bar{\xi}_c)^2 \tag{34}$$

Substitution of the transformations (31) - (34) into Eqns (25) - (29) will verify that the function H indeed satisfies all the requirements (18) - (22). The equality of the ratios $\bar{\xi}_g/\bar{\xi}_c, \bar{\xi}_g/\xi_c, \theta_g/\theta_c$ simplifies the presentation of the results.

The value of G, though theoretically a constant, may be expected to vary somewhat with ξ due to truncation and round-off errors in the solution. It was rather unexpected, however, to find that in certain parameter ranges unacceptable nonuniformities in G were found numerically. However, for those parameter values for which the values of G were sufficiently uniform, the results agreed very well with those of the alternative technique described below.

PRECOMPILER INPUT

The precompiler input corresponding to Eqns. (25) - (29) is shown in Figure A2. The first line identifies the user supplied program name EXTP. This name is used as a prefix in naming subroutines generated by the preprocessor to facilitate readability of the generated program by the user. Next, room is provided for some options. In the present precompiler version, this is superfluous since only one option now exists. Next, one may note in Figure A2 some text enclosed between `/* . . . */`. This text constitutes a comment which is ignored by the precompiler. Following this text, some declarations appear. These declarations categorize identifiers as parameters, independent, dependent and entry names. Parameters signify variables whose numerical value will be read in at run time by a standard read statement. Entry names, not illustrated in Figure A2, are names of library or user defined subroutines, and so on.

Following the preamble, the actual statements of the differential equation (DE), boundary conditions (BC), and initial conditions (IC) are provided. The specification: BC LOW (XIR * XIC, *) means: This is a boundary condition at the low end of the interval of independent variable #1; i.e., X whose value at that point is the expression XIR * XIC[†]. In addition, the BC is valid for any value (*) of independent variable #2, i.e., T. The rest of the input is self-explanatory.

[†]Naturally, this value could have been a constant or a variable name.

```

EXTP:  PROCEDURE OPTIONS(PARABOLIC);
/* EXTERNALLY PRESSURIZED FOIL BEARING ANALYSIS.
STATIONARY, INCOMPRESSIBLE, PLANAR, PERFECTLY
FLEXIBLE, REFERENCED TO A CYLINDRICAL SURFACE.
TWO SOURCES, SYMMETRICALLY LOCATED ABOUT CENTER. */

      DECLARE
XIC  PARAMETER, /* COORDINATE OF CENTER */
XIR  PARAMETER, /* XIG/XIC , WHERE XIG=COORDINATE OF SOURCE */
X18  PARAMETER, /* COORDINATE, END OF LUBRICATION ZONE */
HG   PARAMETER, /* H VALUE AT SOURCE */
HMIN PARAMETER; /* INITIAL VALUE OF H AT TANGENCY POINT */
      DECLARE
X    INDEPENDENT(1), /* 1ST VARIABLE IN LIST, SPATIAL COORDINATE */
T    INDEPENDENT(2), /* 2ND VARIABLE IN LIST, TIME COORDINATE */
H    DEPENDENT; /* DIMENSIONLESS FILM THICKNESS, H_BAR IN PAPER */

DE:      @4X(H)*(-H**3) +@3X(H)*(-3.*H**2*@X(H))=@T(H);
BC LOW (XIR*XIC,*): H=HG;
BC LOW (XIR*XIC,*): @2X(H)*(XIR-1.)*XIC+@X(H)*(-1.)=0.;
BC HIGH (X18,*): @X(H)=X18;
BC HIGH (X18,*): @2X(H)=1.;
IC:      H=HMIN+X**2/2.;

      END;

```

Figure A2 Precompiler Input (Corresponding to Eqns (25)-(29))

PRECOMPILER STRUCTURE

The precompiler is composed of three sub-programs: 1. Lexical analyzer, 2. Syntactic and semantic analyzer; and 3. Synthesizer.

The lexical analyzer consists of a small driver section which picks an input character, decodes it, and branches to several possible routines accordingly. These routines identify literals (e.g., 2.0, 20.E-1, 2), identifiers (e.g., XIR, SQRT), reserved words (e.g., DE, BC), comments, etc. Identifiers and literals are stored in a table. The output of the lexical analyzer is a uniform stream of pairs of descriptors, the first of which indicates the type of element encountered (e.g., **, +, identifier). The second descriptor points, when necessary, to a table of additional information (e.g., the actual identifier's name).

The syntactic/semantic analyzer scans the pairs emitted by the lexical analyzer and parses them. Parsing means, in principle, matching of a precompiler input statement to a set of prototype statements describing the grammar of the input language. For example, the two prototype statements

$$\begin{aligned} \text{assignment} &\Leftarrow \text{variable} = \text{expression} \\ \text{expression} &\Leftarrow \text{term} [+ \text{term}] \end{aligned}$$

where the brackets indicate zero or more repetitions of elements of the enclosed form, may be matched to a fortran statement such as

$$A = B + C$$

Several parsing methods are available in compiler design. Parsing was done in this work by recursive descent [2]. In essence, for each of the grammar nonterminal symbols (e.g., assignment, variable, term), there is a logical recursive subroutine which returns "true" or "false" depending on whether the terminal language symbol

(e.g., A, B, =, +) can be matched to the prototype. A subroutine called "assignment" calls the subroutine "variable"; and if it is true that the symbol is a variable, checks whether the next symbol in the input string is a "=", and so on. This parsing process is continued until the input structure is matched to the syntax rules or else there is no match due to a user grammar error. Once a match is achieved, reference is made to a set of routines which produce the desired output segment for the final high-level language program. For example, since the differential equation is converted into a set of algebraic equations in matrix form, the routines will generate assignment statements for the coefficients.

The synthesis phase collects the segments generated by the syntactic/semantic phase and inserts them into a prearranged program template. The template consists of a high-level language (PLI) program for solution of the desired class of equations by an implicit algorithm. The template consists, basically, of the following slots:

Main program -- a driver routine containing a slot for user input.

Matrix generator -- sets up the coefficient matrix for PDE solution and for BC.

Initializer -- the particular initial conditions are set up.

Output -- fixed format output of PDE solution is set up with some user control over the amount of printout).

The generated program uses a diagonal band matrix solver which is a fixed subroutine. This routine takes as its input the matrix equation and its bandwidth and provides the solution.

With standard catalogued procedures (such as we have developed for OS 360), the operation of the program is quite simple. The input has to be stored in a data set. Data sets may optionally be provided by the user for storing the generated PLI program*, the object program, and the output. The precompiler is written in PLI and is, thus, machine independent for all machines for which PLI compiler is available.

*A listing of the generated computer program is given in Appendix III.

APPENDIX II: O.D.E. SOLUTION

Let Eqns (18) - (22) be reformulated in terms of alternative variables $\hat{H}(\hat{\xi})$, in order to permit solution as an ordinary DE. Later the solution for \hat{H} will be transformed back into $H(\xi)$. The reformulated problem is:

$$\hat{H}^3 \frac{d^3 \hat{H}}{d\hat{\xi}^3} = 1 \tag{35}$$

At $\hat{\xi} = 0$

$$\hat{H} = \hat{H}_g \tag{36}$$

$$\hat{H}' = \hat{H}'_g \tag{37}$$

$$\hat{H}'' = \hat{H}''_g \tag{38}$$

Integration as an initial value problem is terminated when \hat{H}'' tends to approach a constant say \hat{H}''_{∞} . The exact termination value is not critical, but it should be sufficiently large so that $\hat{H}_{\infty}/\hat{H}_g \gg 1$. It may be verified that the conversion

$$H = \hat{H} \cdot (\hat{H}''_{\infty})^{3/5}$$

$$\hat{\xi} = \left(\hat{\xi} - \hat{\xi}_{\infty} - \frac{\hat{H}'_{\infty}}{\hat{H}''_{\infty}} \right) \cdot (\hat{H}''_{\infty})^{4/5}$$

transforms the solution a posteriori to that of the original coordinates. The parameters of the problem which has been solved are found by:

$$\pi_g = 1 - \hat{H}_g' / \hat{H}_\infty''$$

$$\xi_g = \hat{H}_\infty' / \hat{H}_\infty''^{1/5} - \sum_{\infty} \hat{H}_\infty''^{4/5}$$

$$\xi_c = \hat{H}_\infty' / \hat{H}_\infty''^{1/5} - \hat{H}_\infty''^{4/5} \left(\hat{H}_g' / \hat{H}_g'' + \sum_{\infty} \right)$$

$$H_c = H_g - \frac{1}{2} (1 - \pi_g) (\xi_g - \xi_c)^2$$

**APPENDIX III: LISTING OF COMPUTER PROGRAM GENERATED
BY PRECOMPILER**

```

EXTP:  PROCEDURE OPTIONS (MAIN);
                DECLARE
DI$  BINARY FIXED(15,0) INITIAL (1), /*PRINT INCR*/
DX1$ DEC FLOAT(6)  INITIAL(0.1), /*SPATIAL STEP*/
DT1$ DEC FLOAT(6)  INITIAL(0.1), /*TIME STEP */
IK$  BINARY FIXED(15,0) INITIAL(1) , /*PRINT FREQUENCY */
IL$  BIN FIXED(15,0)  INITIAL(1), /*SPATIAL COUNTR LO*/
IH$  BIN FIXED(15,0)  INITIAL(11), /*SPATIAL COUNTER HI*/
JFIN  BINARY FIXED (15,0) INITIAL (1), /*NO OF STEPS*/
JS$  (KLIN$) BINARY FIXED (15,0), /*LINE NUMBER */
KBC$  BINARY FIXED (15,0) INITIAL ( 2), /*HALF BAND OF MATRIX */
KBCP1$ BINARY FIXED (15,0) INITIAL ( 3),
KLIN$ BINARY FIXED (15,0) INITIAL (9), /*LINES STORED*/
ORDER$ BINARY FIXED (15,0) INITIAL ( 4);
L1:  GET DATA (
      XIC,HG,XIR,HMIN,XI8,
      JFIN,IL$,IH$,DI$,DT1$);
      CALL HD_EXTP;
      GO TO L1;

HD_EXTP: PROCEDURE;
                DECLARE
A$  (IL$-ORDER$/2:IH$+ORDER$/2,-ORDER$/2:ORDER$/2+1)
      DEC FLOAT(16), /*MATRIX EQN*/
EMATXP  ENTRY, /*SOLVE MATRIX EQN */
ESTOREP  ENTRY, /*STORE FOR PRINTING*/
EWRITEP  ENTRY , /* PRINT ROUTINE */
H      (1:KLIN$,IL$:IH$) DEC FLOAT(16); /*DEPENDENT VAR*/
A$=0.;
XL$=XIR*XIC;
XH$=XI8;
DX1$=(XH$-XL$)/(IH$-IL$);
PUT DATA (
      XIC,HG,XIR,HMIN,XI8,
      JFIN,IL$,IH$,DI$,DT1$);
PUT DATA (DX1$);
ILP$=IL$+KBC$;
IHM$=IH$-KBC$;
DX2$=DX1$*DX1$;DX3$=DX2$*DX1$;DX4$=DX3$*DX1$;
CALL IC_EXTP;
    
```

```

L2: DO JR$=1 TO JFIN ;
    CALL EQ_EXTP;
    CALL BC_EXTP;
    CALL EMATRX;
    IF (MOD(JR$,IK$)=0) THEN CALL ESTOREP;
    IF((K$=KLIN$) | (JR$=JFIN)) THEN CALL EWRITEP;
    END L2;
    RETURN;

```

```

IC_EXTP: PROCEDURE;
    JR$=0;
    K$=1;
    JS$(K$)=JR$;
    DO I$=IL$ TO IH$;
        H(K$,I$)=HMIN+(I$-IL$)*DX1$**2/2.;
    END;
    RETURN;
END IC_EXTP;

```

```

EQ_EXTP: PROCEDURE;
    DO I$=ILP$ TO IHM$ ;
    C4$=(-H(K$,I$)**3);
    C3$=(-3.*H(K$,I$)**2*(+1./DX1$*H(K$,I$+0)
    ));
    A$(I$,-2)=(+1./DX4$*C4$-.5/DX3$*C3$)*DT1$;
    A$(I$,-1)=(-4./DX4$*C4$+1./DX3$*C3$)*DT1$;
    A$(I$,+0)=(+6./DX4$*C4$+0.*C3$)*DT1$-1.;
    A$(I$,+1)=(-4./DX4$*C4$-1./DX3$*C3$)*DT1$;
    A$(I$,+2)=(+1./DX4$*C4$+.5/DX3$*C3$)*DT1$;
    A$(I$,+3)=-H(K$,I$);
    END;
    RETURN;
END EQ_EXTP;

```

```

BC_EXTP: PROCEDURE;
    A$(IL$,+0)=+1.;
    A$(IL$,+1)=+0.;
    A$(IL$,+2)=0.;
    A$(IL$,KBCP1$)=HG;
    C2$=(XIR-1.)*XIC;
    C1$=(-1.);
    A$(IL$+1,-1)=+2./DX2$*C2$-1.5/DX1$*C1$;
    A$(IL$+1,+0)=-5./DX2$*C2$+2./DX1$*C1$;
    A$(IL$+1,+1)=+4./DX2$*C2$-0.5/DX1$*C1$;
    A$(IL$+1,+2)=-1./DX2$*C2$;
    A$(IL$+1,KBCP1$)=0.;
    A$(IH$,-2)=+0.5/DX1$;
    A$(IH$,-1)=-2./DX1$;
    A$(IH$,+0)=+1.5/DX1$;
    A$(IH$,KBCP1$)=X18;
    A$(IH$-1,-2)=-1./DX2$;
    A$(IH$-1,-1)=+4./DX2$;
    A$(IH$-1,+0)=-5./DX2$;
    A$(IH$-1,+1)=+2./DX2$;
    A$(IH$-1,KBCP1$)=1.;
    RETURN;
END BC_EXTP;

```

```

EMATRX:  PROCEDURE;
          DECLARE
            (I$,KH$,KV$)  BINARY FIXED (15,0); /*LOOP INDICES */
PS1: DO I$=IL$ TO IH$;
      DO KH$=1 TO KBCP1$;
        A$(I$,KH$)= A$(I$,KH$)/A$(I$,0);
      DO KV$=1 TO KBC$;
        IF (KH$=KBCP1$)
          THEN A$(I$+KV$,KBCP1$)=A$(I$+KV$,KBCP1$)
            -A$(I$,KBCP1$)*A$(I$+KV$,-KV$);
        ELSE A$(I$+KV$,KH$-KV$)=A$(I$+KV$,KH$-KV$)
            -A$(I$,KH$)*A$(I$+KV$,-KV$);
      END;
    END;
  END PS1;
PS2: DO I$=IH$ TO IL$+1 BY -1;
      DO KV$=1 TO KBC$;
        A$(I$-KV$,KBCP1$)=A$(I$-KV$,KBCP1$)
            -A$(I$,KBCP1$)*A$(I$-KV$,KV$);
      END;
    END PS2;
  RETURN;
END EMATRX;

```

```

ESTOREP:  PROCEDURE;
          DECLARE
            IC      BINARY FIXED (15,0) ;
            K$=1+ MOD(K$,KLIN$);
            JS$(K$)=JR$;
            DO I$=IL$ TO IH$;
              H(K$,I$)= A$(I$,KBCP1$);
            END;
          RETURN;
        END ESTOREP;

```

```

EWRITEP:  PROCEDURE;
          DECLARE
            (IC,KC)      BINARY FIXED (15,0);
            PUT EDIT ('I$/JS$',(JS$(IC) DO IC=1 TO K$))
              (COL(1),A(6),(K$) F(12,0), SKIP(2));
            DO IC=IL$ TO IH$ BY DI$;
              PUT EDIT (IC,(H(KC,IC) DO KC=1 TO K$))
                (COL (1),F(6,0), (K$) E(12,4));
            END;
          PUT PAGE;
          RETURN;
        END EWRITEP;

        END HD_EXTP;
        END EXTP;

```

REFERENCES

1. A. Eshel and H. G. Elrod Jr., "The Theory of the Infinitely Wide, Perfectly Flexible, Self-Acting Foil Bearing." J. Basic Engrg., Trans. ASME, Ser D, Vol. 87, Dec. 1965, pp. 831-836.
2. D. Gries, "Compiler Construction for Digital Computers". Wiley, 1971.

DISTRIBUTION LIST FOR UNCLASSIFIED
TECHNICAL REPORTS ISSUED UNDER
CONTRACT NO0014-71-C-0001 TASK NR 062-297

All addressees receive one copy unless otherwise specified

Defense Documentation Center
Cameron Station
Alexandria, VA 22314

12 copies

Mr. Stanley L. Zedekar
Dept. 244-2, Bldg. 71
Autonetics
P. O. Box 4181
Anaheim, CA 92803

Technical Library
David W. Taylor Naval Ship Research
and Development Center
Annapolis Laboratory
Annapolis, MD 21402

Professor Bruce Johnson
Engineering Department
Naval Academy
Annapolis MD 21402

Library
Naval Academy
Annapolis, MD 21402

Professor C. S. Yih
Department of Engineering Mechanics
University of Michigan
Ann Arbor, MI 48105

Dr. Coda Pan
Shaker Research Corporation
Northway 10 Executive Park
Ballston Lake, NY 12019

NASA Scientific and Technical Information
Facility
P. O. Box 8757
Baltimore/Washington International Airport
Maryland 21240

Director
Office of Naval Research Branch Office
495 Summer Street
Boston, MA 02210

Commander
Puget Sound Naval Shipyard
Bremerton, WA 98314

Dr. Alfred Ritter
CALSPAN Corporation
P. O. Box 235
Buffalo, NY 14221

Commanding Officer
NROTC Naval Administrative Unit
Massachusetts Institute of Technology
Cambridge, MA 02139

Professor J. Nicholas Newman
Department of Ocean Engineering
Room 5-324A
Massachusetts Institute of Technology
Cambridge, MA 02139

Library
C.S. Draper Laboratory
68 Albany Street
Cambridge, MA 02139

Professor A. R. Kuhlthau, Director
Research Laboratories for the Engineering
Sciences
Thornton Hall
University of Virginia
Charlottesville, VA 22903

Dr. Edgar J. Gunter, Jr.
University of Virginia
School of Engineering and Applied
Science
Charlottesville, VA 22903

Director
Office of Naval Research Branch Office
536 South Clark Street
Chicago, IL 60605

Professor L. N. Tao
Illinois Institute of Technology
Chicago, IL 60616

Library
Naval Weapons Center
China Lake, CA 93555

Mr. W. J. Anderson
NASA Lewis Research Center
Cleveland, OH 44871

Commander
Charleston Naval Shipyard
Naval Base
Charleston, SC 29408

Mr. J. W. Kannel
Sattelle Memorial Institute
505 King Avenue
Columbus, OH 43201

Technical Library
Naval Weapons Surface Center
Dahlgren Laboratory
Dahlgren, VA 22418

Professor A. McKillop
Department of Mechanical Engineering
University of California
Davis, CA 95616

Mr. H. M. Anderson
Xerox Data Systems
701 South Aviation Boulevard
El Segundo, CA 90245

Professor Ralph Burton
Department of Mechanical Engineering
and Astronautical Sciences
Northwestern University
Evanston, IL 60210

Dr. Martin H. Bloom
Director of Gas Dynamics Research
Polytechnic Institute of New York
Long Island Center
Farmingdale, NY 11735

Mr. L. R. Manoni
Manager, Advanced Programs
United Aircraft Corporation Systems
Center
1690 New Britain Avenue
Farmington, CT 06023

Research & Technology Division
Army Engineering Reactors Group
Fort Belvoir, VA 22060

Technical Documents Center
Building 315
Army Mobility Equipment Research Center
Fort Belvoir, VA 22060

Technical Library
Webb Institute of Naval Architecture
Glen Cove, NY 11542

Mr. Richard P. Shevchenko
Pratt and Whitney Aircraft Corporation
East Hartford, CT 06108

Dr. J. P. Breslin
Davidson Laboratory
Stevens Institute of Technology
Castle Point Station
Hoboken, NJ 07030

Mr. P. H. Broussard, Jr.
Guidance and Control Division
National Aeronautics & Space Administration
George C. Marshall Space Flight Center
Huntsville, AL 35812

Professor J. F. Kennedy, Director
Institute of Hydraulic Research
University of Iowa
Iowa City, IA 52242

Professor William K. Stair
Assistant Dean, Mechanical and
Aerospace Engineering
University of Tennessee
Knoxville, TN 37916

Professor J. Modrey
School of Mechanical Engineering
Purdue University
Lafayette, IN 47907

Professor A. T. Ellis
Department of Applied Mathematics
and Engineering Sciences
University of California, San Diego
La Jolla, CA 92037

Professor W. Lindberg
Department of Mechanical Engineering
University of Wyoming
Laramie, WY 82070

Mr. Otto Decker
Mechanical Technology, Incorporated
968 Albany-Shaker Road
Latham, NY 12110

Mr. Virgil Johnson, President
Hydronautics, Incorporated
7210 Pindell School Road
Laurel, MD 20810

Commander
Long Beach Naval Shipyard
Long Beach, CA 90801

Lorenz G. Straub Library
St. Anthony Falls Hydraulic Laboratory
University of Minnesota
Minneapolis, MN 55414

Mr. K. Liebler, Supervisor
Head & Media Development
Control Data Corporation
Normandale Division
7801 Computer Avenue
Minneapolis, MN 55424

Professor Paul F. Pucci
Mechanical Engineering Department
Naval Postgraduate School
Monterey, CA 93940

Library
Naval Postgraduate School
Monterey, CA 93940

Technical Library
Naval Underwater Systems Center
Newport, RI 02840

Office of Naval Research
New York Area Office
715 Broadway - Fifth Floor
New York, NY 10003

Professor D. D. Fuller
Department of Mechanical Engineering
Columbia University
New York, NY 10027

Professor V. Castelli
Department of Mechanical Engineering
Columbia University
New York, NY 10027

Professor H. G. Elrod
Department of Mechanical Engineering
Columbia University
New York, NY 10027

Engineering Societies Library
345 East 47th Street
New York, NY 10017

Society of Naval Architects and
Marine Engineers
74 Trinity Place
New York, NY 10006

Mr. Ralph F. DeAngelias
Norden Division of United Technology
Research Center
Helen Street
Norwalk, CT 06852

Mr. Anthony W. Lawrence
Northrop Corporation
Electronics Division
100 Morse Street
Norwood, MA 02062

Mr. R. G. Jordan
Oak Ridge Gaseous Diffusion Pl.
Union Carbide Corporation - Nuclear
Division
P. O. Box P
Oak Ridge, TN 37830

Mr. R. E. MacPherson
Oak Ridge National Laboratory
P. O. Box Y
Oak Ridge, TN 37831

Technical Library
Naval Coastal System Laboratory
Panama City, FL 32401

Director
Office of Naval Research Branch Office
1030 E. Green Street
Pasadena, CA 91101

Technical Library
Naval Ship Engineering Center
Philadelphia Division
Philadelphia, PA 19112

Technical Library
Philadelphia Naval Shipyard
Philadelphia, PA 19112

Mr. Wilbur Shapiro, Manager
Friction and Lubrication Laboratory
The Franklin Institute Research Laboratories
The Benjamin Franklin Parkway
Philadelphia, PA 19103

Dr. F. Osterle
Department of Mechanical Engineering
Carnegie Institute of Technology
Pittsburgh, PA 15213

Technical Library
Naval Missile Center
Point Mugu, CA 93041

Commander
Portsmouth Naval Shipyard
Portsmouth, NH 03801

Commander
Norfolk Naval Shipyard
Portsmouth, VA 23709

Chief, Document Section
Redstone Scientific Information Center
Army Missile Command
Redstone Arsenal, AL 35809

Dr. A. Eshel
Ampex Corporation
401 Broadway
Redwood City, CA 94063

Mr. M. Wildmann
Ampex Corporation
401 Broadway
Redwood City, CA 94063

Army Research Office
P. O. Box 12211
Research Triangle Park, NC 27709

ONR Scientific Liaison Group
American Embassy - Room A-407
APO San Francisco 96503

Editor
Applied Mechanics Review
Southwest Research Institute
8500 Culebra Road
San Antonio, TX 78206

Dr. J. W. Hoyt
Code 2501
Naval Undersea Center
San Diego, CA 92132

Technical Library
Naval Undersea Center
San Diego, CA 92132

Office of Naval Research
San Francisco Area Office
760 Market Street, Room 447
San Francisco, CA 94102

Library
Pearl Harbor Naval Shipyard
Box 400
FPO San Francisco 96610

Technical Library
Hunters Point Naval Shipyard
San Francisco, CA 94135

Professor Bruce H Adee
Department of Mechanical Engineering
University of Washington
Seattle, WA 98195

Mr. C. C. Moore, Manager
Reliability and Safety Engineering
Gas Turbine Division
General Electric Company
Schenectady, NY 12345

Librarian
Naval Surface Weapons Center
White Oak Laboratory
Silver Spring, MD 20910

Fenton Kennedy Document Library
The Johns Hopkins University
Applied Physics Laboratory
John Hopkins Road
Laurel, MD 20310

Mr. Graham Patterson
Admiralty Compass Observatory
Ditton Park
Slough, Bucks, England

Mr. Steve Rohrbough
Honeywell Inc., Aerospace Division
13350 U.S. Highway 19
St. Petersburg, FL 33733

Mr. Roland Baldwin
Section Head - Inertial Components
Honeywell Inc., Aerospace Division
13350 U.S. Highway 19
St. Petersburg, FL 33733

Professor R. DiPrima
Department of Mathematics
Rensselaer Polytechnic Institute
Troy, NY 12181

Dr. L. A. Segel
Department of Mathematics
Rensselaer Polytechnic Institute
Troy, NY 12181

Walt Tucker
Nuclear Engineering Department
Brookhaven National Laboratory
Upton, Long Island, NY 11973

Technical Library
Mare Island Naval Shipyard
Valleno, CA 94592

Mr. E. Roland Maki
Mechanical Development Department
General Motors Corporation
12 Mile and Mound Roads
Warren, MI 48090

Office of Naval Research
Code 438
800 N. Quincy Street
Arlington, VA 22217

3 copies

Office of Naval Research
Code 200
800 N. Quincy Street
Arlington, VA 22217

Office of Naval Research
Code 210
800 N. Quincy Street
Arlington, VA 22217

Office of Naval Research
Code 211
800 N. Quincy Street
Arlington, VA 22217

Office of Naval Research
Code 212
800 N. Quincy Street
Arlington, VA 22217

Office of Naval Research
Code 221
800 N. Quincy Street
Arlington, VA 22217

Office of Naval Research
Code 473
800 N. Quincy Street
Arlington, VA 22217

Office of Naval Research
Code 480
800 N. Quincy Street
Arlington, VA 22217

Office of Naval Research
Code 481
800 N. Quincy Street
Arlington, VA 22217

Office of Naval Research
Code 1021P (ONRL)
800 N. Quincy Street
Arlington, VA 22217

Code 2627
Naval Research Laboratory (6 copies)
Washington, DC 20375

Code 4000
Naval Research Laboratory
Washington, DC 20375

Code 7706
Naval Research Laboratory
Washington, DC 20375

Mr. L. Benen (Code 0322)
Naval Sea Systems Command
Washington, DC 20362

Mr. J. Schuler (Code 032)
Naval Sea Systems Command
Washington, DC 20362

Code 03B
Naval Sea Systems Command
Washington, DC 20362

Mr. T. Peirce (Code 03512)
Naval Sea Systems Command
Washington, DC 20362

Library (Code 09GS)
Naval Sea Systems Command
Washington, DC 20362

Code 6034
Naval Ship Engineering Center
Center Building
Prince George's Center
Hyattsville, MD 20782

Code 6101E
Naval Ship Engineering Center
Center Building
Prince George's Center
Hyattsville, MD 20782

Code 6110
Naval Ship Engineering Center
Center Building
Prince George's Center
Hyattsville, MD 20782

Code 6114
Naval Ship Engineering Center
Center Building
Prince George's Center
Hyattsville, MD 20782

Code 6136
Naval Ship Engineering Center
Center Building
Prince George's Center
Hyattsville, MD 20782

Code 6140
Naval Ship Engineering Center
Center Building
Prince George's Center
Hyattsville, MD 20782

Dr. A. Powell (Code 01)
David W. Taylor Naval Ship
Research and Development Center
Bethesda, MD 20084

6 copies

Mr. W. M. Ellsworth (Code 11)
David W. Taylor Naval Ship Research
and Development Center
Bethesda, MD 20084

Dr. W. E. Cummins (Code 15)
David W. Taylor Naval Ship Research
and Development Center
Bethesda, MD 20084

Library (Code 5641)
David W. Taylor Naval Ship Research
and Development Center
Bethesda, MD 20084

Code 03
Naval Air Systems Command
Washington, DC 20361

Code 03B
Naval Air Systems Command
Washington, DC 20361

Code 310
Naval Air Systems Command
Washington, DC 20361

Code 5301
Naval Air Systems Command
Washington, DC 20361

Strategic Systems Projects Office
Department of the Navy
Washington, DC 20376

Mr. Norman Nilsen (SP 2022)
Strategic Systems Projects Office
Department of the Navy
Washington, DC 20376

Oceanographer of the Navy
200 Stovall Street
Alexandria, VA 22332

Commander
Naval Oceanographic Office
Washington, DC 20373

Dr. A. L. Slafkosky
Scientific Advisor
Commandant of the Marine Corps (Code AX)
Washington, DC 20380

Librarian Station 5-2
Coast Guard Headquarters
NASSIF Building
400 Seventh Street, SW
Washington, DC 20591

Office of Research and Development
Maritime Administration
441 G Street, NW
Washington, DC 20235

Division of Ship Design
Maritime Administration
441 G Street, NW
Washington, DC 20235

Air Force Office of Scientific
Research/NA
Building 410
Bolling AFB
Washington, DC 20332

AFDRD-AS/M
U.S. Air Force
The Pentagon
Washington, DC 20330

Chief of Research and Development
Office of Chief of Staff
Department of the Army
Washington, DC 20310

Headquarters Library
Energy Research & Development
Administration
Washington, DC 20545

Mr. Clarence E. Miller, Jr.
Division of Reactor Development
and Technology
Energy Research and Development
Administration
Washington, DC 20545

Mr. W. M. Crim
Office of Coal Research
Energy Research and Development
Administration
Washington, DC 20545

National Science Foundation
Engineering Division
1800 G Street, NW
Washington, DC 20550

Science and Technology Division
Library of Congress
Washington, DC 20540

Professor J. V. Foa
School of Engineering and Applied
Science
George Washington University
Washington, DC 20006

Defense Research and Development Attache
Australian Embassy
1601 Massachusetts Avenue, NW
Washington, DC 20036

Mr. Everett Lake (APFL)
AF Aero Propulsion Laboratory
Wright-Patterson AFB, OH 45433

Mr. S. Abramovitz
Abramovitz Associates Inc.
P. O. Box 393
Bronxville, NY 10708

